Alginate Lyase Aly36B is a New Bacterial Member of the Polysaccharide Lyase Family 36 and Catalyzes by a Novel Mechanism With Lysine as Both the Catalytic Base and Catalytic Acid

Fang Dong[1], Fei Xu[1], Xiu-Lan Chen[1,2], Ping-Yi Li[1], Chun-Yang Li[2,3], Fu-chuan Li[1], Yin Chen[3,4], Peng Wang[1,3] and Yu-Zhong Zhang[1,2,3]

*1 - **State Key Laboratory of Microbial Technology,** Marine Biotechnology Research Center, Shandong University, Qingdao, 266237, China*

*2 - **Laboratory for Marine Biology and Biotechnology,** Pilot National Laboratory for Marine Science and Technology (Qingdao), Qingdao, 266237, China*

*3 - **College of Marine Life Sciences,** Institute for Advanced Ocean Study, Ocean University of China, Qingdao, 266003, China*

*4 - **School of Life Sciences,** University of Warwick, Coventry, CV4 7AL, United Kingdom*

***Correspondence to Peng Wang and Yu-Zhong Zhang:** State Key Laboratory of Microbial Technology, Marine Biotechnology Research Center, Shandong University, Qingdao, 266237, China; State Key Laboratory of Microbial Technology, Marine Biotechnology Research Center, Shandong University, Qingdao, 266237, China.*
wangwanlue@163.com, zhangyz@sdu.edu.cn
https://doi.org/10.1016/j.jmb.2019.10.023

Abstract

Alginate lyases, which are important in both basic and applied sciences, fall into ten polysaccharide lyase (PL) families. PL36 is a newly established family that includes 39 bacterial sequences and one eukaryotic sequence. Till now, the structures or catalytic mechanisms of PL36 alginate lyases have yet to be revealed. Here, we characterized a novel PL36 alginate lyase, Aly36B, from *Chitinophaga* sp. MD30. Aly36B is a polymannuronate specific endolytic alginate lyase. To probe the catalytic mechanism of Aly36B, the structures of wild-type Aly36B and its mutants (K143A/Y185A in complex with alginate tetrasaccharide and K143A/M171A with trisaccharide) were solved. The overall structure of Aly36B belongs to the β-jelly roll scaffold, adopting a typical β-sandwich fold. Aly36B contains a Ca^{2+}, which is far away from the active center and plays an important role in stabilizing the structure of Aly36B. Based on structural and mutational analyses, the catalytic mechanism of Aly36B for alginate degradation was explained. During catalysis, Arg^{169}, Tyr^{185}, and Tyr^{187} are responsible for neutralizing the negative charge of the substrate, and Lys^{143} acts as both the catalytic base and the catalytic acid, which represents a new kind of catalytic mechanism of alginate lyases. Sequence alignment shows that these four residues involved in catalysis are highly conserved in all PL36 sequences, suggesting that PL36 alginate lyases may adopt a similar catalytic mechanism. Taken together, this study reveals the molecular structure and catalytic mechanism of a PL36 alginate lyase, broadening our knowledge on alginate lyases and facilitating future biotechnological applications of PL36 alginate lyases.

Introduction

Brown algae are abundant in the sea, especially in coastal environments, which are an important nutrient source for heterotrophic organisms. Alginate is a linear polysaccharide present in the cell walls and intercellular material of brown algae, accounting for ~40% of their dry weight [1–3]. Alginate consists of two monomeric units, β-D-mannuronate (M) and its C5 epimer α-L-guluronate (G). These two units may be arranged following three patterns: polyguluronate (PG), polymannuronate (PM), and heteropolymeric random sequences (PMG) [4,5]. Some bacteria belonging to the *Pseudomonas* and *Azotobacter* genera also produce alginate. Bacterial alginates differ from those produced by brown

algae in that they have little or no G-blocks and can be O-acetylated at some of the C-2 and C-3 carbons of the mannuronic acid residues [6–8].

Alginate lyases catalyze the degradation of alginate, targeting the glycosidic 1, 4 O-linkage via acid-base catalysis of β-elimination [9]. Alginate lyases are grouped into α-L-guluronosyl linkage-specific lyases (EC 4.2.2.11, G-specific), β-D-mannuronosyl linkage-specific lyases (EC 4.2.2.3, M-specific) and bifunctional lyases according to their different substrate specificities. In the Carbohydrate-Active enZYmes (CAZY) database, alginate lyases fall into ten polysaccharide lyase (PL) families (PL5, 6, 7, 14, 15, 17, 18, 32, 34, and 36) [10–12], among which families PL32, 34, and 36 were established just recently according to the research of Helbert et al.[12]. The three-dimensional structures of some alginate lyases have been solved, which can be grouped into three scaffolds: β-jelly rolls (PL7, 14, and 18), right-handed β-helix fold (PL6) and (α/α)n toroid fold (PL5, 15, and 17) [13–22]. Based on structural and biochemical analyses, the catalytic mechanisms of some alginate lyases have been revealed. Generally, alginate lyases adopt two types of catalytic mechanisms: the alginate lyases from families PL5, 7, 14, 15, 17, and 18 adopt the His (or Tyr)/Tyr elimination mechanism [11,13,14,16–22], and the alginate lyase AlyGC from family PL6 adopts the metal-assisted elimination mechanism [15]. In addition to their ecological role in natural alginate degradation, alginate lyases have been shown to be important in biotechnological applications [23,24]. For examples, alginate lyases are used to prepare alginate oligomers and to assist the treatment of chronic bacterial infection via their effective degradation of the exopolysaccharides in bacterial biofilm [25,26]. In recent years, it has been shown that alginate lyases have promising potential in commercial-scale fuel ethanol production from brown algal alginate [27].

To date, the newly established family PL36 includes 40 amino acid sequences that are annotated as PL36 alginate lyases in the CAZy database, which all but one eukaryotic sequence (ABS82817.1) originate from bacteria. The endomannuronan lyase (H600DRAFT_04136) from *Flavobacterium denitrificans* DSM 15936 is an M-specific endolytic alginate lyase [12], and is the only characterized enzyme of this family. Till now, the structures or the catalytic mechanisms of PL36 alginate lyases have yet to be revealed.

In this study, the characteristics, structure and catalytic mechanism of a PL36 alginate lyase was studied. The *aly36B* gene (GenBank accession No. NZ_CP023254.1) from the bacterium *Chitinophaga* sp. MD30 was predicted to encode a PL36 alginate lyase. The *aly36B* gene was overexpressed in *Escherichia coli* and the recombinant enzyme Aly36B was characterized to be an endotype M-specific alginate lyase, mainly producing disaccharides from PM. Moreover, the structures of wild-type (WT) Aly36B (2.3 Å resolution) and its mutants K143A/Y185A in complex with M4 (2.3 Å resolution) and K143A/M171A with M3 (2.8 Å resolution) were solved. Based on structural and mutational analyses, the endolytic reaction mechanism of Aly36B for substrate catalysis was explained, which showed that Aly36B adopts a new kind of catalytic mechanism different from those reported on the other alginate lyases. The results provide a foremost insight into the characteristics, structure, and catalytic mechanism of a PL36 alginate lyase, offering a better understanding of the catalytic mechanisms of alginate lyases for alginate depolymerization.

Results and Discussion

Characterization of Aly36B

The *aly*36B gene from *Chitinophaga* sp. MD30 is 882 bp in length and predicted to encode a PL36 alginate lyase (Aly36B) of 293 amino acid residues. Aly36B contains a 34-residue signal peptide (predicted by SignalP 4.0) and a catalytic domain (Ala^{35}-Arg^{293}). Aly36B shares 49% identity with the endomannuronan lyase (H600DRAFT_04136) from *Flavobacterium denitrificans,* the only characterized alginate lyase in family PL36 [12]. In addition, Aly36B shares low identities to some PL14 alginate lyases. For example, Aly36B shares 26% identity to vAL-1 (covering 55% of the Aly36B sequence) and 26% identity to AkAly30 (covering 55% of the Aly36B sequence). vAL-1 and AkAly30 are two PL14 alginate lyases whose structures were solved.

To characterize Aly36B, it was overexpressed in *E. coli* BL21 (DE3) without the signal peptide and purified. The recombinant Aly36B with a predicted molecular mass of 28.45 kDa showed the maximal activity toward sodium alginate at 35 °C (Fig. 1a) and pH 9.0 (Fig. 1b). The salt-tolerant ability of Aly36B is quite low, displaying the highest activity in 0 M NaCl and losing almost 100% activity in 2 M NaCl (Fig. 1c). Among sodium alginate, PM and PG, Aly36B showed the highest activity toward PM but little activity toward PG, indicating that Aly36B is an M-specific enzyme (Fig. 1d), similar to the PL36 endomannuronan lyase (H600DRAFT_04136) and the PL14 alginate lyases AkAly30, LbAly28, and HdAly[11,12]. The K_m values of Aly36B were 0.46 ± 0.08 mg/ml towards sodium alginate, and 0.30 ± 0.10 mg/ml toward PM (Table 1), which are similar to those of AkAly30 [18]. Thin-layer chromatography (TLC) analysis showed that the products released from PM degradation by Aly36B were mainly disaccharides (Fig. 1e) and a minority of monosaccharides and oligosaccharides with degree of

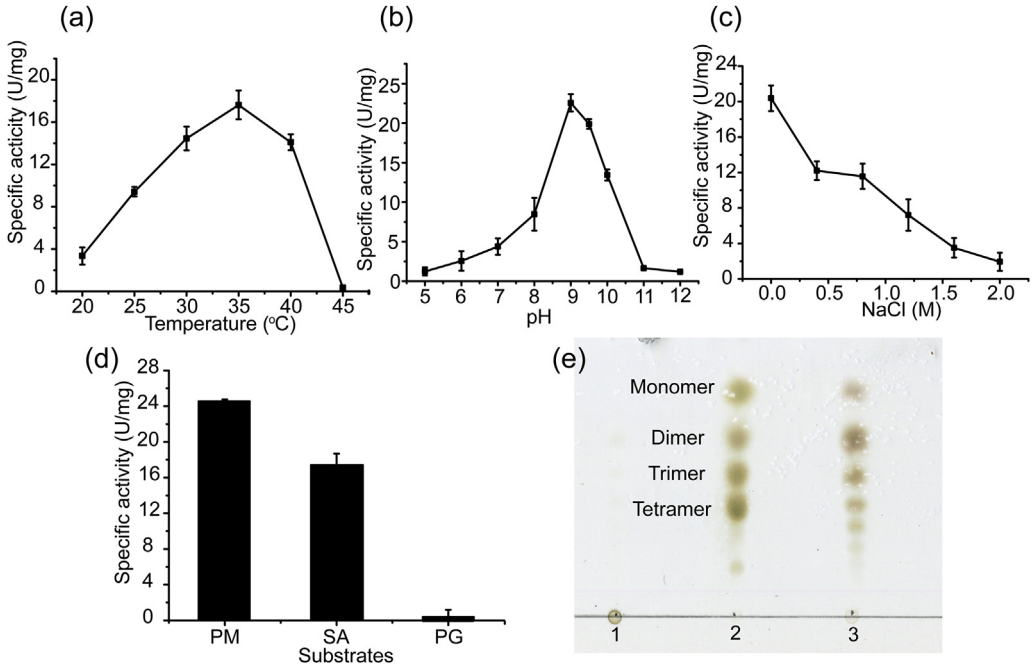

Fig. 1. Biochemical characterization of Aly36B. (a) The effect of temperature on Aly36B activity. (b) The effect of pH on Aly36B activity. Experiments were performed at 35 °C in 50 mM Britton-Robinson buffer ranging from pH 5 to 12. (c) The effect of NaCl on Aly36B activity. Assays in A, B, and C were carried out with sodium alginate as the substrate. (d) Substrate specificities of Aly36B toward sodium alginate (SA), polymannuronate (PM), and polyguluronate (PG). Experiments were conducted in a 200 μl mixture containing 100 μg/ml enzyme and 2 mg/ml substrate in 50 mM Tris-HCl (pH 9.0) at 35 °C for 10 min. (e) TLC analysis of the degradation products of Aly36B on PM. A 200 μl reaction mixture containing 50 μg/ml enzyme and 2 mg/ml PM was incubated at 35 °C for 12 h. Lane 1, PM. Lane 2, monomannuronic acid, dimannuronic acid, trimannuronic acid and tetramannuronic acid standards. Lane 3, the degradation products from PM by Aly36B. The data shown in (a)−(d) are from triplicate experiments (mean ± standard deviation [SD]). The figure shown in (e) is a representative of triplicate experiments.

polymerization >2, indicating that Aly36B is an endolytic alginate lyase, similar to the PL36 endo-mannuronan lyase (H600DRAFT_04136) [12].

Overall structure of Aly36B

To study the catalytic mechanism of Aly36B for alginate cleavage, we solved the crystal structure of WT Aly36B by single-wavelength anomalous dispersion method using a selenomethionine derivative (Se derivative). The crystal of WT Aly36B belongs to the P 2 21 21 space group and the structure was determined to a 2.3 Å resolution (Table 2). Structure data show that each asymmetric unit contains one Aly36B molecule of 241 residues (Ala^{52}−Arg^{293}) (the N-terminal 18 residues are disordered in the structure probably because of flexibility) (Fig. 2a). Gel filtration result suggests that Aly36B presents as a monomer in solution (Fig. 2b). Aly36B adopts a typical β-sandwich fold structure that is composed of an α-helix, two large β-sheets (sheet A and sheet B) and four short loops (L1, L2, L3, L4) (Fig. 2a). Sheet A and sheet B consist of five and eight β-strands, respectively (Fig. 2a). Among the three scaffolds that alginate lyases adopt [11], the three-dimensional structure of Aly36B belongs to the β-jelly roll scaffold. This scaffold is also adopted by alginate lyases from families PL7, 14 and 18, such as the PL7 enzymes A1-II′ (PDB code:2ZAB) [16], the PL14 enzymes AkAly30 (PDB code: 5GMT) [18] and vAL-1 (PDB code: 3GNE) [19], and the PL18 enzyme Aly SJ02 (PDB code: 5GMT) [22].

Among alginate lyase structures, the topological structure of Aly36B is most similar to those of vAL-1 and AkAly30 from family PL14 [18,19] (Fig. 3a). There is a positively charged groove in the middle of Aly36B. It is surrounded by two Loops (L1, L2) and three β-strands of sheet A (A2, A4, A5). Tyr^{195} on L1 and Ser^{270} on L2 are located at the top of the groove and their interaction makes the subsite −1 closed (Fig. 3b), which is similar to AkAly30 but different from vAL-1 whose groove is open (Fig. 3b). One phosphate (PO_4^{3-}) ion from the crystallization buffer is accommodated in the positively charged groove and interacts with the residues Lys^{143}, Arg^{169}, Tyr^{185}, and Tyr^{187} (Fig. 2a).

Structural analysis shows that there is a metal ion-binding site in the structure of WT Aly36B, which is

Table 1. Kinetic parameters of Aly36B and its mutants.[a]

Enzyme	Substrate	K_m (mg/ml)	V_m (U/mg)
WT	PM	0.30 ± 0.10	24.90 ± 2.79
WT	alginate	0.46 ± 0.08	18.69 ± 1.33
R140A	PM	11.69 ± 0.96	13.24 ± 0.88
Y173A	PM	3.21 ± 0.87	14.89 ± 2.07

[a] The kinetic parameters of the mutants with an activity <5% activity of WT Aly36B (Fig. 6a) could not be determined due to their low activity.

Table 2. Diffraction data and refinement statistics of WT Aly36B, SeMet Aly36B, K143A/Y185A-M4, and K143A/M171A-M3.

Parameters	WT Aly36B	SeMet Aly36B	K143A/Y185A-M4	K143A/M171A-M3
Data collection				
Space group	P 2 21 21	P 1 21 1	C 2 2 21	C 2 2 21
Unit cell				
a, b, c (Å)[a]	53.77	55.02	105.58	105.77
	89.49	96.73	187.53	188.32
	46.86	63.53	91.69	91.11
α, β, γ (°)	90.00	90.00	90.00	90.00
	90.00	93.60	90.00	90.00
	90.00	90.00	90.00	90.00
Wavelength (Å)	0.9791	0.9791	0.9791	0.9791
Resolution (Å)	46.86–2.28 (2.28–2.38)	47.76–2.30 (2.3–2.38)	93.77–2.28 (2.38–2.28)	40.84–2.79 (2.89–2.79)
Redundancy	5.3 (5.2)	6.8 (6.7)	10.1 (9.9)	4.5 (4.9)
Completeness (%)	97.0 (99.1)	99.9 (99.9)	98.0 (99.9)	97.2 (98.6)
R_{merge}[b]	0.137 (0.339)	0.139 (0.309)	0.120 (0.250)	0.183 (0.395)
I/sigma	25.06 (8.33)	30.50 (11.77)	37.45 (13.38)	15.20 (5.71)
Refinement statistics				
Resolution (Å)	46.86–2.28 (2.28–2.38)		35.34–2.28 (2.28–2.36)	40.84–2.79 (2.89–2.79)
R_{work} (%)	19.64 (26.14)		16.60 (17.48)	19.76 (22.68)
R_{free} (%)	23.36 (43.03)		20.06 (26.00)	27.10 (31.44)
B-factor (Å^2)				
Protein	43.22		28.75	22.72
Solvent	40.67		34.11	28.25
Ligands	48.68		35.94	20.30
Rmsd from ideal geometry				
Rmsd length (Å)	0.008		0.012	0.0015
Rmsd angles (°)	1.20		1.02	1.35
Ramachandran Plot (%)[c]				
Favored	95.04%		95.87%	93%
Allowed	4.96%		3.44%	6.4%

[a] Numbers in parentheses refer to data in the highest resolution shell.
[b] $R_{merge} = \Sigma_{hkl}\Sigma_i|I(hkl)_i - \langle I(hkl)\rangle| / \Sigma_{hkl}\Sigma_i \langle I(hkl)_i\rangle$.
[c] The Ramachandran plot was calculated by PROCHECK program in CCP4i program package.

chelated by residues Asn^{62}, Asn^{64}, Gly^{96}, and Asp^{286}, as well as two water molecules (Fig. 4a). The coordination geometry and electron density intensity suggest that the ion is likely Ca^{2+}. Inductively coupled plasma optical emission spectrometry (ICP-OES) analysis also showed that ~1.0 Ca^{2+} was present per Aly36B molecule. Thus, the ion-binding site is assigned as Ca^{2+}. The Ca^{2+} binding site is far away from the active center of Aly36B (Fig. 2a). Consequently, removing the Ca^{2+} from Aly36B by ethylenediaminetetraacetic acid (EDTA) had little effect on the enzymatic activity (Fig. 4b). However, apo-Aly36B without Ca^{2+} showed significant decreases in the enzyme thermostability at 25 °C and 30 °C compared with the WT (Fig. 4c), suggesting that Ca^{2+} plays an important role in the stabilization of the protein structure of Aly36B. Sequence alignment suggests that some PL36 alginate lyases have a similar metal ion binding site as Aly36B and the Ca^{2+} binding residues are partly conserved in these alginate lyases (Fig. 4d). This suggests that these PL36 alginate lyases may contain a metal ion, similar to Aly36B. However, in the reported structures of the PL14 alginate lyases, neither vAL-1 nor AkAly30 contains a metal ion (Supplementary Fig. S1) [18,19].

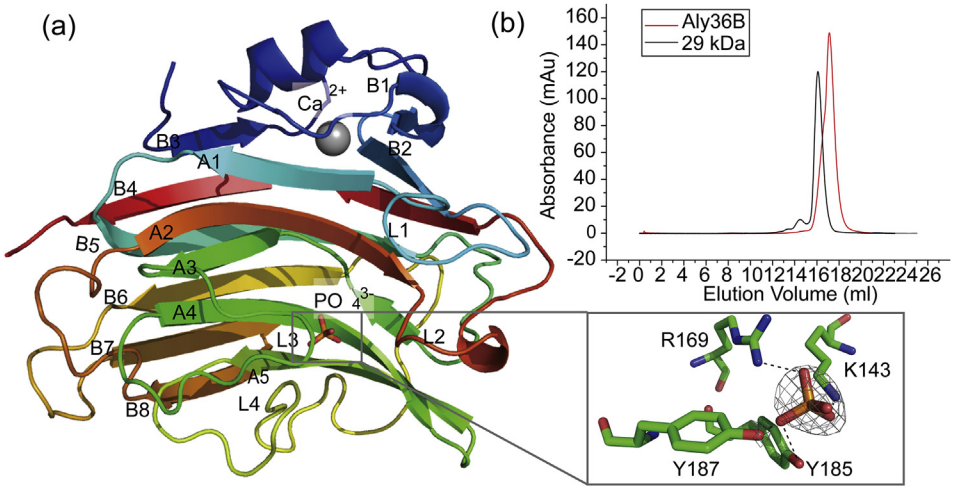

Fig. 2. The overall structure of Aly36B. (a) The overall structure of WT Aly36B. 2Fo-Fc omit electron density (2.0 σ) of the ions. The 2Fo-Fc densities for PO_4^{3-} are contoured in brown at 1.5σ. (b) Gel filtration analysis of Aly36B in solution. Carbonic anhydrase (29 kDa) was used as the size standard.

Important residues for substrate recognition and catalysis in Aly36B

To solve the structure of Aly36B in complex with a substrate molecule, we performed mutations to inactivate Aly36B and obtained three inactive mutants, K143A, K143A/M171A, and K143A/Y185A. These mutants were tried to cocrystallize with M oligosaccharides. Finally, the crystal structures of K143A/Y185A in complex with an M4 molecule (K143A/Y185A-M4, 2.3 Å resolution) and K143A/M171A in complex with an M3 molecule (K143A/M171A-M3, 2.8 Å resolution) were solved, whereas the quality of the crystals of K143A with the substrate was not good enough for data collection and structural analysis.

The structures of K143A/M171A-M3 and K143A/Y185A-M4 show root mean square deviations of 0.41 Å and 0.35 Å, respectively, to that of WT Aly36B (Fig. 5a and b). The structures of K143A/Y185A-M4 and K143A/M171A-M3 show a root mean square deviation of only 0.28 Å. Structural alignment of the three structures shows that the positions of the residues in the active center are similar in these structures and that the conformations of the M3 molecule in K143A/M171A-M3 and the M4 molecule in K143A/Y185A-M4 are the same (Fig. 5a and b).

The M3/M4 chain is labeled with *-n* to represent the nonreducing terminus and *+n* to respect the reducing terminus (Fig. 5a and b). As shown in Fig. 5c, the M4 molecule is bound in the positively charged tunnel of Aly36B. The catalytic tunnel is open at two ends, which is corresponding to its endolytic character (Fig. 5c). The positive charge of the tunnel is beneficial for the binding of the negatively charged alginate chain.

Alginate tetrasaccharide was mainly cleaved into dimers by Aly36B (Fig. 5d), suggesting that the cleavage mainly occurs between the −1 and +1 site of the M4 molecule. Alginate cleavage is a typical acid-base catalysis of β-elimination reaction. The β-elimination catalytic mechanism requires neutralization of the negative charge on the +1 site carboxylic group [11]. Around the +1 subsite, three residues, Arg^{169}, Tyr^{185}, and Tyr^{187}, are conserved in the PL36 alginate lyases (Fig. 7b). These residues interact with the carboxyl group of the +1 site mannose molecule (Fig. 5a). When Arg^{169}, Tyr^{185}, or Tyr^{187} was mutated to alanine, the mutants lost the activity toward PM (Fig. 6a and b). These results suggest that Arg^{169}, Tyr^{185}, and Tyr^{187} are responsible for neutralizing the negative charge on the +1 site carboxylic group, just as the role of Arg^{239} and Asn^{191} in alginate lyase A1-III [13,14].

Catalytic acid and catalytic base are essential for alginate lyases in the alginate β-elimination [11]. Structural alignment of WT Aly36B, K143A/M171A-M3, and K143A/Y185A-M4 suggests that only one hydrophilic residue, Lys^{143}, which is conserved in PL36 alginate lyases, is close to both the +1 site C_5 and -1 site O_4 of the M4/M3 molecule (Fig. 5a). Mutation of Lys^{143} to Ala (K143A) inactivated Aly36B (Fig. 6a and b). When Lys^{143} was modeled into the active site of K143A/M171A-M3 according to its position in WT Aly36B, the distance between Lys^{143} and the +1 site C_5 of M3 is 2.88 Å, and the interactions of Lys^{143} with Gly^{268} and Met^{171} may reduce the pK_a of Lys^{143} (Figs. 5d and 6a). Therefore, Lys^{143} is likely to act as the catalytic base in the acid-base catalysis of Aly36B for alginate degradation. In addition, the distance between Lys^{143} and the +1 site O_4 of M3 is 2.65 Å, making it possible for

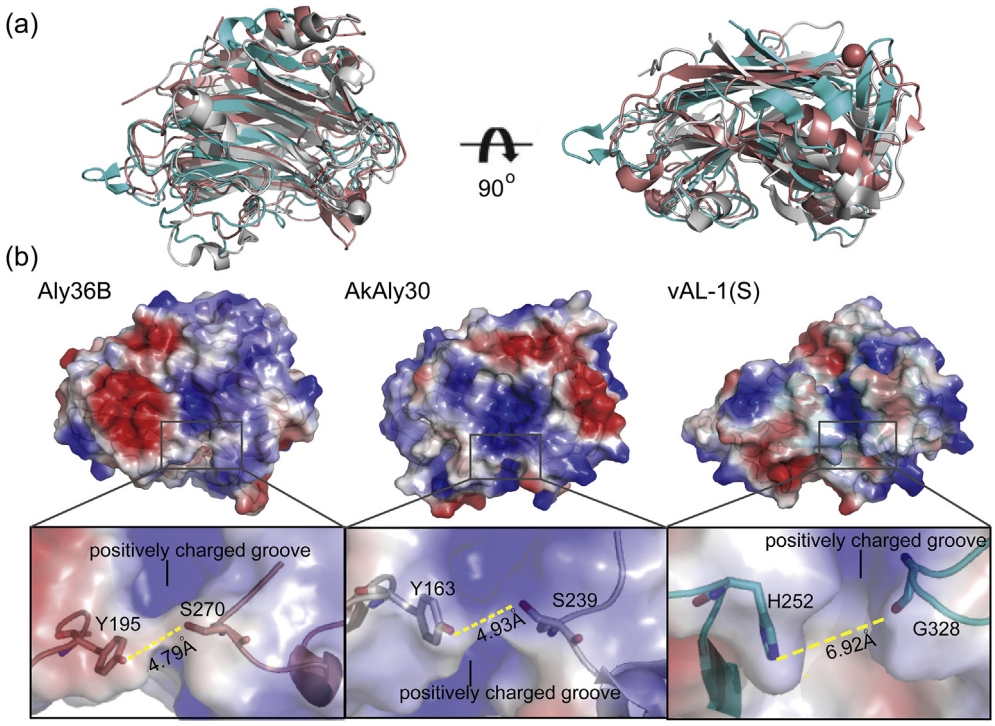

Fig. 3. Structure comparison of Aly36B, AkAly30, and vAL-1(s). (a) Structure alignment of alginate lyases Aly36B, AkAly30, and vAL-1(s). AkAly30 is in silver, Aly36B in pink, and vAL-1(s) in blue. (b) Comparison of the positively charged grooves of Aly36B, AkAly30, and vAL-1(s).

Lys^{143} to act as the catalytic acid. In K143A/M171A-M3, Tyr^{185}, whose position is the same as that in WT Aly36B, also points toward the +1 site C_5. However, the distance between the hydroxyl of Tyr^{185} and the +1 site C_5 of M3 is more than 4.0 Å and the distance between Tyr^{185} and the +1 site O_4 of M3 is more than 3.0 Å (Fig. 5a). Therefore, though Tyr^{185} has the potential to participate in proton transfer, Lys^{143} is more likely to be the catalytic base and acid owing to its closer distances to the +1 site C_5 and -1 site O_4. Thus, Lys^{143} in Aly36B likely plays the same role as the catalytic residue tyrosine (acting as both the catalytic base and the catalytic acid) in the PL5 alginate lyase A1-III [13,14] and the PL18 alginate lyase aly-SJ02 [22]. The lysine residue has been reported to function as a catalytic base in the polysaccharide lyases from PL3, 6, 9, 11, and 28 (Supplementary Fig. S2) [15,28–31] and is also suggested to be the catalytic acid in the PL3 pectin lyase PelI [28].

We also studied the functions of other residues that interact with the M3/M4 molecule by mutational and biochemical analyses. When residues Arg^{140} and Tyr^{173}, which interact with the −2 site carboxyl group of the M3/M4 molecule, were mutated to Ala, the K_m values of the mutants were all significantly increased (Fig. 6a and b, Table 1), suggesting that these residues are responsible for substrate recognition.

Catalytic mechanism of the PL36 alginate lyase Aly36B

Based on the above structural and biochemical results, the catalytic mechanism of Aly36B for alginate degradation was proposed. Aly36B depolymerizes alginate through a β-elimination reaction between the subsites −1 and +1 sites. Four residues in the active center of Aly36B, Lys^{143}, Arg^{169}, Tyr^{185}, and Tyr^{187}, which are highly conserved in family PL36, are key residues involved in catalysis (Fig. 5a, Supplementary Fig. S3). When the substrate enters the active center, Arg^{169}, Tyr^{185}, and Tyr^{187} interact with the carboxyl group of the +1 site mannuronic acid to neutralize the negative charge and activate the C_5 proton (Fig. 7a). Lys^{143} functions as a catalytic base to attack the C_5 proton of the +1 site mannuronic acid, leading to the formation of an enolate intermediate. Subsequently, the redundant electron is transferred back to Lys^{143} from the glycoside bond, leading to the cleavage of the O-glycosidic bond and the formation of the C4=C5 double bond. Finally, the oligosaccharide products are released from the catalytic site, and

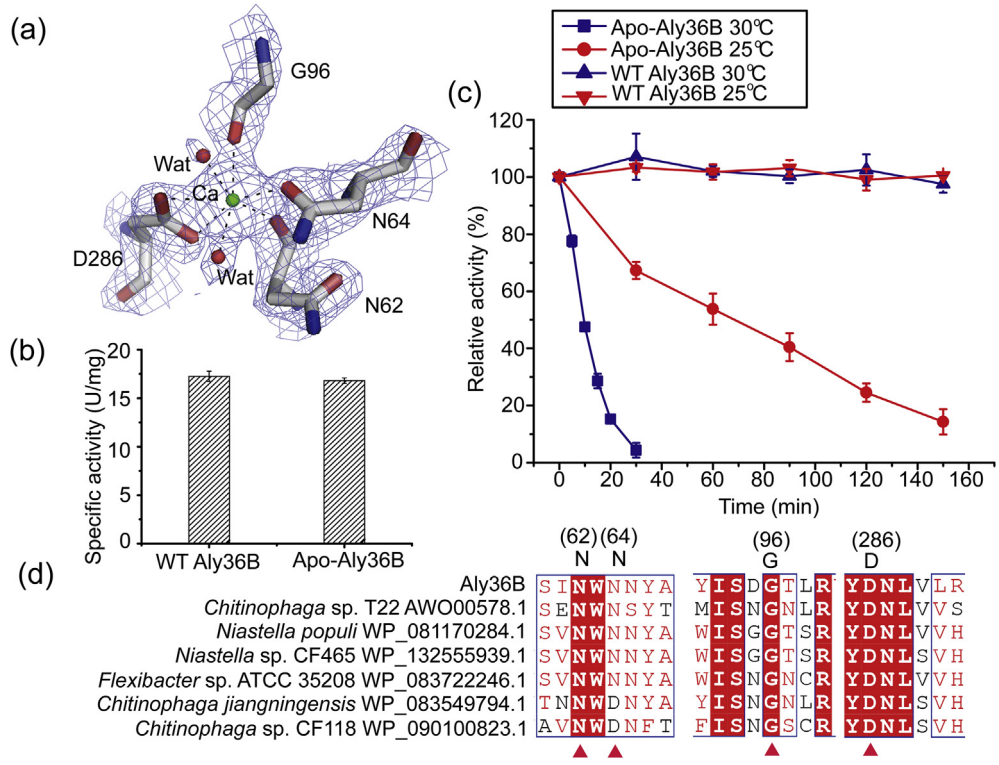

Fig. 4. Function analysis of Ca^{2+} in Aly36B. (a) The binding site of the Ca^{2+} ion in Aly36B. The 2Fo-Fc densities for Ca^{2+} and the binding residues are contoured in blue at 1.5σ. (b) The activities of WT Aly36B and Apo-Aly36B. Apo-Aly36B was prepared by the addition of 5 mM EDTA followed by desalination to remove Ca^{2+}. (c) The thermostability of WT Aly36B and Apo-Aly36B at 25 °C and 30 °C. (d) Sequence alignment of PL36 alginate lyases. Red triangles indicate the residues that are involved in Ca^{2+} coordination. The data shown in (b) and (c) are from triplicate experiments (mean ± standard deviation [SD]).

Aly36B is ready to catalyze the cleavage of another substrate (Fig. 7a).

Alignment of all the sequences that have been assigned to family PL36 in the CAZy database shows that the catalytic key residue Lys^{143}, and the essential residues involved in negative charge neutralization (Arg^{169}, Tyr^{185}, and Tyr^{187}) in Aly36B are highly conserved in the PL36 alginate lyases (Fig. 7b). This result suggests that the catalytic mechanism of Aly36B revealed in this study is likely a common catalytic mechanism adopted by the PL36 alginate lyases.

Comparison of the catalytic mechanism of Aly36B with those of the other alginate lyases

Among alginate lyases of the other families, the PL36 Aly36B has the highest similarity to those in PL14. The catalytic mechanism of the PL14 alginate lyase AkAly30 has been explained based on a molecular docking model with a M4 molecule. The overall structures of Aly36B and AkAly30 are similar (Fig. 3a), and the spatial arrangement of the four key residues Lys^{143}, Arg^{169}, Tyr^{185}, and Tyr^{187} of Aly36B are also similar to those of AkAly30, with a root mean square deviation of 0.17 Å (Fig. 8). However, we noticed that the binding mode of the substrate molecule in Aly36B is different from that in the AkAly30 model (Fig. 8), the substrate molecule being bound in the opposite direction in Aly36B and AkAly30. In the AkAly30 model with M4, Lys^{99} interacts with the carboxyl group at subsite +1 and Tyr^{140} locates near both the C_5 atom at subsite −1 and the glycosidic O atom between subsite −1 and +1. Therefore, Tyr^{140} and Lys^{99} were predicted as the key residues for the reaction, Tyr^{140} was proposed as the general base and proton donor, and Lys^{99} was suggested to neutralize the negative charge [24]. In Aly36B complexed with M3/M4, Lys143 (equivalent to Lys^{99} in AkAly30) locates near both the C_5 atom at subsite −1 and the glycosidic O atom between subsite −1 and +1, and Tyr^{185} (equivalent to Tyr^{140} in AkAly30) points towards the carboxyl group at subsite +1. Thus, Lys^{143} is most likely to act as the general base and proton donor, and Tyr185 may assist the proton transfer in Aly36B. Therefore, the difference in

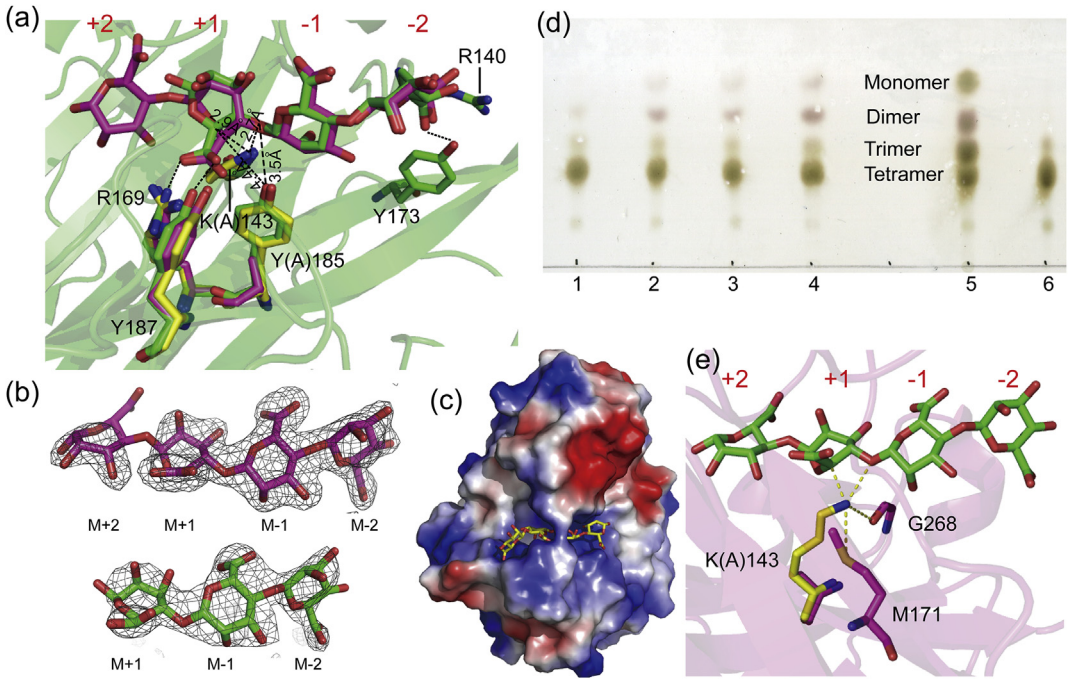

Fig. 5. Analyses of the important amino acid residues in the active center of Aly36B. (a) Structural alignment of active center of WT Aly36B, K143A/Y185A-M4, and K143A/M171A-M3. The residues in the WT structure are presented as yellow sticks. The residues and the M3 molecule in the K143A/M171A-M3 complex are presented as green sticks. The residues and the bound M4 from −2 to +2 subsites in the K143A/Y185A-M4 complex are presented as purple sticks. (b) Fo-Fc omit maps of the M4 molecule in the K143A/Y185A-M4 complex and the M3 molecule in the K143A/M171A-M3 complex. The simulated annealing Fo-Fc omit maps were generated using the Phenix program by omitting the M3 and M4 molecules. The resulting electron density maps were contoured at 3 sigma and superimposed with the final M3 and M4 models. (c) Electrostatic surface view of the K143A/Y185A-M4 complex. The M4 molecule is shown as yellow sticks. (d) Thin-layer chromatography (TLC) analysis of the degradation products of Aly36B on tetramannuronic acid. A 200 μl reaction mixture containing 50 μg/ml enzyme and 2 mg/ml tetramannuronic acid was incubated at 35 °C. Lane 1, 5 min; Lane 2, 30 min; Lane 3, 60 min; Lane 4, 120 min; Lane 5, monomannuronic acid, dimannuronic acid, trimannuronic acid, and tetramannuronic acid standards; Lane 6, tetramannuronic acid standard. The main products released from PM degradation by Aly36B were disaccharides. The figure shows a representative of triplicate experiments. (e) The hydrogen bonds between Lys^{143} and Met^{171}, Gly^{268}, and the M4 molecule. The hydrogen bonds are represented by dotted lines.

substrate binding mode may lead to the different catalytic mechanisms of Aly36B and AkAly30.

Alginate lyases from different PL families adopt three different scaffolds: β-jelly rolls (PL7, 14, and 18), right-handed β-helix fold (PL6), and (α/α)n toroid fold (PL5, 15, and 17) [13–22]. Moreover, the arrangements of the catalytic residues in the active centers of alginate lyases from different PL families

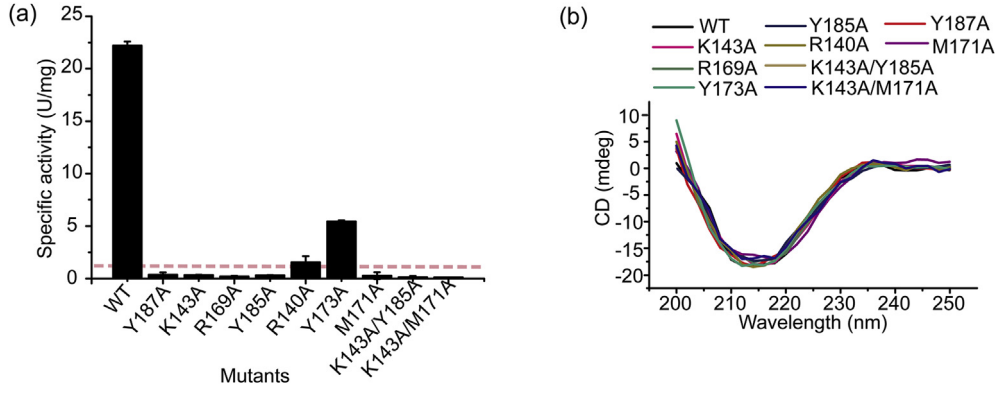

Fig. 6. Mutational analysis of important residues in the active site of Aly36B. (a) Enzymatic activities of Aly36B mutants toward polymannuronate (PM). The dotted line shows 5% activity of WT Aly36B. (b) CD spectra of Aly36B and its mutants.

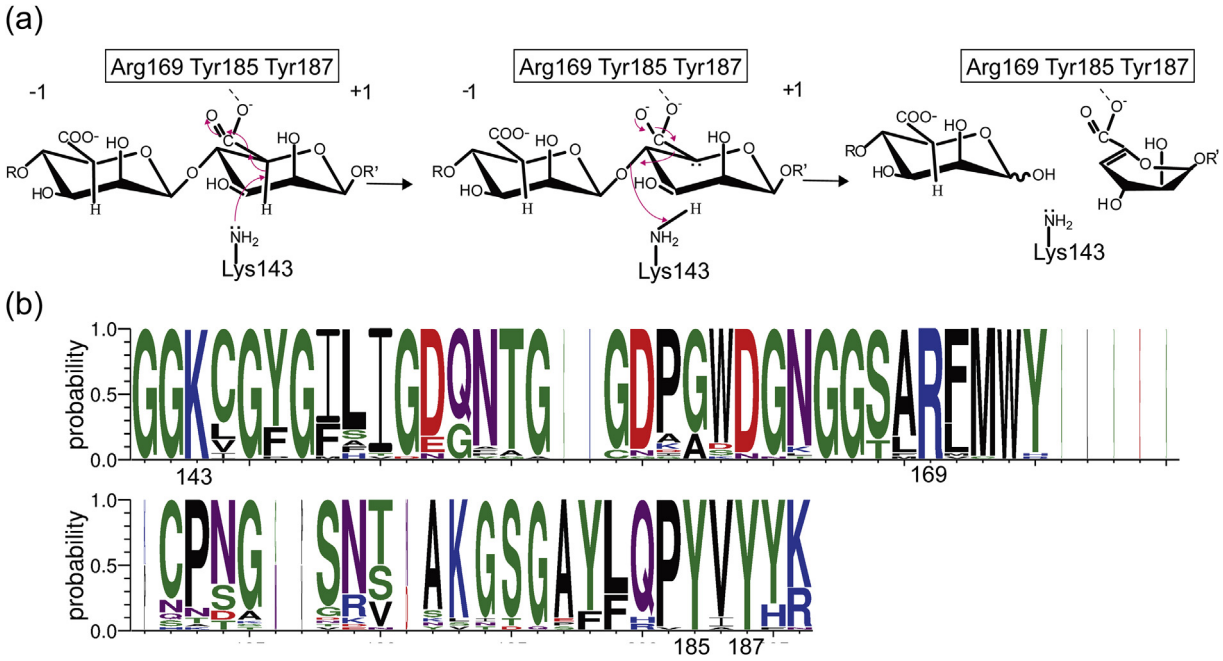

Fig. 7. Proposed mechanism of alginate depolymerization by Aly36B. (a) The catalytic mechanism of Aly36B. Arg^{169}, Tyr^{185}, and Tyr^{187} form interactions with the carboxyl group of the +1 site mannuronic acid to neutralize the negative charge and activate the C_5 proton. Lys^{143} functions as a catalytic base to abstract the proton at C5 and then receive the redundant electron from the glycoside bond. (b) An overview of conservation residues involved in catalysis of PL36 alginate lyases. Residues are numbered according to Aly36B. Sequence logos were made using WebLogo (http://weblogo.threeplusone.com).

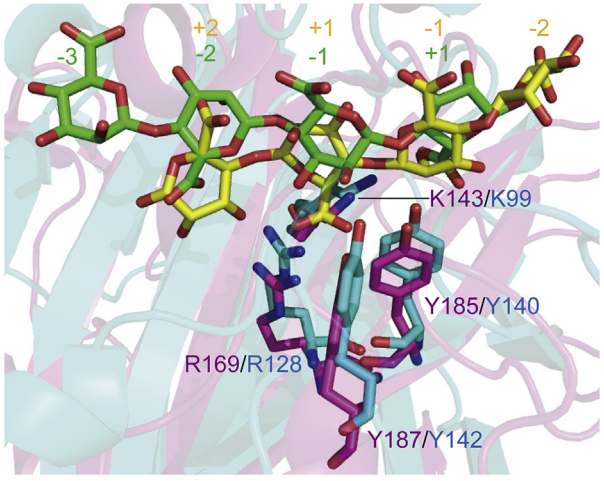

Fig. 8. The active center comparison of Aly36B and AkAly30. The catalytic residues in Aly36B are presented as purple sticks, and the bound M4 from +2 to −2 subsites is shown as yellow sticks. The catalytic residues in AkAly30 are presented as cyan sticks, and the bound M4 from −3 to +1 subsites is shown as green sticks [24].

are quite different (Fig. 9a), which may lead to the diversity of the catalytic mechanisms of alginate lyases. The catalytic mechanisms of alginate lyases have been generally divided into two types [11,32]: The first type uses a metal ion to neutralize the acidic group. This metal-assisted β elimination is so far adopted by only the PL6 family alginate lyase AlyGC, in which Ca^{2+} neutralizes the C-5 carboxyl negative charge, a Lys residue functions as the base and an Arg residue functions as the acid [15]. The second type uses residues (Glu, His, Arg, or Asn) to neutralize the acidic group, in which Tyr acts as the catalytic base and Tyr or His as the catalytic acid [11,32]. Except AlyGC, all the other alginate lyases adopt the second type of catalytic mechanism. This type is further divided into two kinds: the first kind uses the same one residue to serve as both the general base and the general acid, and the second kind uses two residues to serve as the general base and the general acid, respectively [32]. The alginate lyases from families PL5, 14, and 18 adopt the first kind, all using a Tyr residue for both the proton acceptor and proton donor [13,14,22]. The alginate lyases from PL7, 15, and 17 adopt the second kind: the alginate lyases from PL7 and 15 use His as the proton acceptor and Tyr as the proton donor [16,20], and the PL17 alginate lyase Alg17c uses Tyr^{450} as the catalytic base and Tyr^{258} as the catalytic acid [21]. Thus, alginate lyases with the same scaffold may adopt different kinds of catalytic mechanism, and vice versa. Consistently, although the PL36 Aly36B has a similar β-jelly roll scaffold as the

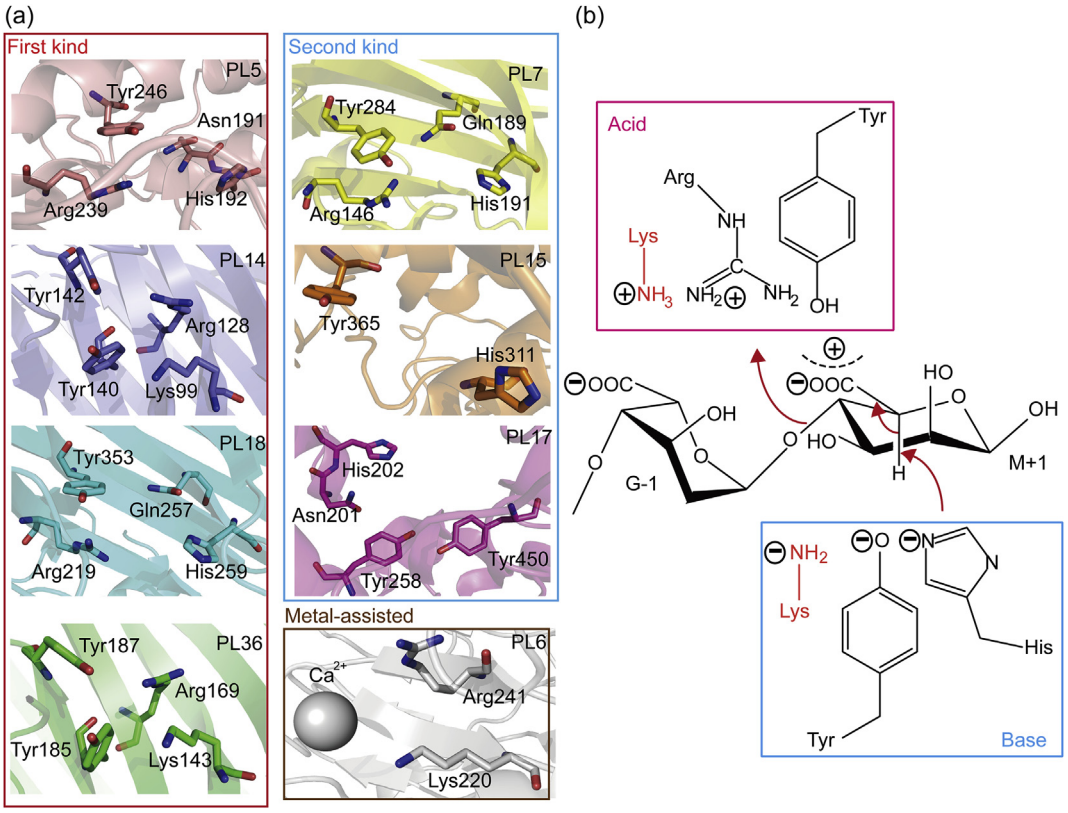

Fig. 9. Comparison of the arrangement of catalytic residues and the catalytic mechanisms of alginate lyases. (a) Conformational comparison of the catalytic residues in the alginate lyase active centers. PL5 alginate lyase A1-III (1HV6) is in pink, PL6 alginate lyase AlyGC (5GKD) in silver, PL 7 alginate lyase A1-II' (2ZAB) in yellow, PL14 alginate lyase AkAly30 (5GMT) in blue, PL15 alginate lyase Atu3025 (3A0O) in wheat, PL17 alginate lyase Alg17c (4NEI) in purple, PL18 alginate lyase aly-SJ02 (4Q8K) in cyan, and PL36 alginate lyase Aly36B (6KCV) in green. (b) Schematic diagram of the catalytic mechanisms adopted by alginate lyases. Tyr/Arg/Lys functions as a catalytic acid, and Tyr/His/Lys functions as a catalytic base.

alginate lyases from PL7 and 18 [16,22], the arrangement of the catalytic residues of Aly36B is quite different from those of the PL7 and 18 alginate lyases (Fig. 9a), which may result in the different catalytic mechanisms of these alginate lyases. The PL36 Aly36B uses a Lys residue as both the catalytic base and the catalytic acid, different from the alginate lyases from families PL7 and 18. Therefore, the Lys/Lys elimination adopted by Aly36B is a new catalytic mechanism in the first kind of the second β elimination type of alginate lyases (Fig. 9a and b).

Although PL36 is a newly established family, the number of alginate lyase sequences in this family has reached 40, which would be increasing in the future due to the discovery of new alginate lyase sequences. Undoubtedly, the PL36 alginate lyases play a role in environmental alginate degradation and recycling. In this study, our results reveal the characteristics, structure, and catalytic mechanism of a PL36 alginate lyase and indicate that the PL36 alginate lyase adopts a new kind of catalytic mechanism for alginate degradation. This study sheds new light on the structures and catalytic mechanisms of alginate lyases. The results will also facilitate the development and biotechnological applications of PL36 alginate lyases in the future.

Experimental Procedures

Gene synthesis and site-directed mutagenesis

The *aly36B* gene from the genome of *Chitinophaga* sp. MD30 was synthesized by the Beijing Genomics Institute (China). The *aly36B* gene without the 34-residue signal peptide sequence was cloned into the vector pET-22b for protein expression. Site-directed mutations were carried out by a modified QuikChange TM site-directed mutagenesis method using plasmid pET22b-*aly36B* as the template [33]. All recombinant plasmids were verified by sequencing.

Protein expression and purification

Recombinant proteins of WT Aly36B and its mutants were overexpressed in *E. coli* BL21 (DE3), which were

induced by 0.3 mM isopropyl β-D-1-thiogalactopyranoside (IPTG) at 15 °C for 16 h. Selenomethionine (SeMet)-labeled protein was produced by inhibiting the methionine biosynthesis in *E. coli* BL21 (DE3). Cells grown overnight in the LB medium were collected by centrifugation and the pellet was resuspended in the M9 medium supplemented with 100 mg/l of lysine, phenylalanine, and threonine, 50 mg/l of isoleucine, leucine, and valine, 5.2% (w/v) glucose, and 0.65% (w/v) yeast nitrogen base (YNB). When cell growth reached ~0.6 of OD_{600} at 37 °C, the culture was cooled to 15 °C and 50 mg/l L-selenomethionine was added [34]. Then, protein expression was induced at 15 °C for 16 h by adding 0.4 mM IPTG to the medium.

To purify the recombinant proteins, the *E. coli* cells were collected and disrupted by sonication in 50 mM Tris-HCl buffer (pH 8.0) containing 100 mM NaCl. The recombinant proteins were first purified by nickel-nitrilotriacetic acid resin (Qiagen) and then by gel filtration chromatography on a Superdex 200 column (GE Healthcare) eluted with 10 mM Tris-HCl (pH 8.0) containing 100 mM NaCl. Carbonic anhydrase (29 kDa) from GE Healthcare, which was used as a protein size standard, was calibrated in the same buffer on the column.

Bioinformatics

Multiple sequence alignment was carried out using MUSCLE [35]. SignalP 4.0 was used to identify the potential signal peptide sequence [36].

Biochemical characterization of Aly36B and its mutants

The concentrations of Aly36B and its mutants were determined by a BCA protein assay kit (Thermo Fisher Scientific, America). The activity of Aly36B and its mutants was measured by the ultraviolet absorption spectrometry method [37]. The reaction system (200 μl) contained 50 mM Tris-HCl buffer (pH 9.0), 2 mg/ml of the substrate, and 100 μg/ml of enzyme. The mixture was incubated at 35 °C for 10 min. The reaction was terminated by boiling for 10 min. The alginate lyase activity was measured by monitoring the absorbance of the reaction solution at 235 nm (A235), indicating the production of unsaturated uronic acids as the lyase cleaves the glycosidic bonds in the polymer chain. One unit of enzyme activity was defined as the amount of enzyme which was required for an increase of A235 by 0.1 per min. The optimum temperature for Aly36B activity was determined in a range of 20−45 °C at pH 9.0. The optimum pH for Aly36B activity was determined at 35 °C in 50 mM Britton-Robinson buffer ranging from pH 5.0 to 12.0. The effect of NaCl on Aly36B activity was determined at NaCl concentrations ranging from 0 to 2.0 M. Substrate specificity of Aly36B was tested by measuring its activities toward PM, PG, and sodium alginate. The products released from PM by Aly36B were assayed using TLC. Standards consisted of mono-, di-, tri-, and tetramannuronic acids. The reaction products were separated using a solvent system of *n*-butyl alcohol: formic acid: water (4:6:1, v/v/v) and visualized by incubating the TLC plates at 90 °C for 15 min after spraying with 10% (v/v) sulfuric acid in ethanol.

Enzyme kinetics assays were carried out in 50 mM Tris-HCl buffer (pH 9.0) at 35 °C using PM or sodium alginate at concentrations from 0.05 to 48 mg/ml. Kinetic parameters were calculated by nonlinear regression fit directly to the Michaelis-Menten equation using the Origin8 software. The metal ions in Aly36B were quantified using ICP-OES [38]. Apo-Aly36B was prepared by the addition of 5 mM EDTA followed by desalination. For the thermal stability assay, the enzyme was preincubated at 25 °C and 30 °C for 0−150 min, and the residual activity was measured at 35 °C.

The overall secondary structures of WT Aly36B and its mutants at a concentration of 0.5 mg/ml in 50 mM Tris-HCl buffer (pH 8.0) were monitored at 25 °C on a J-810 circular dichroism (CD) spectropolarimeter (JASCO, Japan). CD spectra were collected from 200 to 250 nm at a scanning rate of 200 nm/min with a path length of 0.1 cm.

All experiments were performed in triplicate, and error was reported as the standard deviation.

Crystallization and data collection

The purified Aly36B protein was concentrated to ~10 mg/ml in 10 mM Tris-HCl (pH 8.0) containing 100 mM NaCl. Crystals of WT Aly36B were obtained at 18 °C using the sitting drop method in the buffer containing 100 mM potassium phosphate monobasic/sodium phosphate dibasic (pH 6.2), 10% (w/v) polyethylene glycol (PEG) 8,000, and 200 mM sodium chloride. Crystals of SeMet-Aly36B were obtained at 18 °C in the buffer containing 100 mM HEPES-NaOH (pH 7.0) and 15% (w/v) PEG 20000. The inactive mutants K143A/Y185A mixed with tetramannuronic acids (1:10) and K143A/M171A mixed with trimannuronic acids (1:10) were crystallized at 18 °C by the hanging drop method in the buffer containing 200 mM potassium phosphate dibasic, 20% (w/v) PEG 3350 after 2 weeks' incubation. All the X-ray diffraction data were collected on the BL17U1 Beam line at Shanghai Synchrotron Radiation Facility using Area Detector Systems Corporation Quantum 315r. The initial diffraction data sets were processed by the HKL2000 program. Relevant data collection is shown in Table 2.

Structure determination, and refinement

The structure of WT Aly36B was determined by single-wavelength anomalous dispersion phasing using a selenomethionine derivative (Se derivative). Heavy atoms were searched by SHELXD [39]. The phase problems were solved by single-wavelength anomalous diffraction (SAD) method using Phenix program Autosol[40]. Initial model building was finished by Phenix program AutoBuild [40]. Refinement of the WT Aly36B structure was done by Phenix program Refine [40] and Coot [41] alternately. The crystal structures of the K143A/Y185A-M4 complex and K143A/M171A-M3 complex were determined by molecular replacement using the CCP4 program Phaser with the structure of WT Aly36B as the search model. The refinement of the structure was performed using Coot and Phenix. The quality of the final model was summarized in Table 2. All structure figures were generated using the PyMOL software [40,41].

Accession codes

The atomic coordinates and structure factors of Aly36B (codes 6KCV, 6KZK, and 6KCW) have been deposited in the Protein Data Bank (PDB) (http://wwpdb.org/).

Acknowledgments

We thank the staffs from BL18U1&BL19U1 beamlines of National Facility for Protein Sciences Shanghai (NFPS) and Shanghai Synchrotron Radiation Facility, for assistance during data collection. The work was supported by the National Science Foundation of China (grants 31870052, 41676180, 31630012, 31670038, 91751101), National Key R&D Program of China (grants 2018YFC0310704, 2018YFC1406700, and 2018YFC1406706), AoShan Talents Cultivation Program Supported by Qingdao National Laboratory for Marine Science and Technology (2017ASTCP-OS14, QNLM2016ORP0310), Taishan Scholars Program of Shandong Province (2009TS079), and the Young Scholars Program of Shandong University (2017WLJH57).

Author Contributions

F.D. and F.X. performed all experiments. X.C. and P.W. directed the experiments. F.D., P.W. and X.C. wrote the manuscript. P.W., C.L. and P.L. solved the structures, and analyzed the data. Y.Z. and X.C. designed the research. Y.C. and F.L. edited the manuscript.

Conflict of Interest

The authors declare no competing financial interests.

Appendix A. Supplementary data

Supplementary data to this article can be found online at https://doi.org/10.1016/j.jmb.2019.10.023.

Received 29 August 2019;
Received in revised form 25 October 2019;
Accepted 27 October 2019
Available online 1 November 2019

Keywords:
alginate lyases;
catalytic mechanism;
PL36 family;
endolytic enzyme;
polymannuronate specific lyase

Abbreviations used:
PL, polysaccharide lyase; M, β-D-mannuronate; G, α-L-guluronate; PDB, Protein Data Bank; M4, D-tetramannuronic acid tetrasodium salt; PG, polyguluronate; PM, polymannuronate.

References

[1] S. Mabeau, B. Kloareg, Isolation and analysis of the cell-walls of Brown-algae - fucus-spiralis, fucus-ceranoides, fucus-vesiculosus, fucus-serratus, bifurcaria-bifurcata and laminaria-digitata, J. Exp. Bot. 38 (1987) 1573–1580.
[2] O.A. Aarstad, A. Tondervik, H. Sletta, G. Skjak-Braek, Alginate sequencing: an analysis of block distribution in alginates using specific alginate degrading enzymes, Biomacromolecules 13 (2012) 106–116.
[3] Y. Zhu, F. Thomas, R. Larocque, N. Li, D. Duffieux, L. Cladiere, F. Souchaud, G. Michel, M.J. McBride, Genetic analyses unravel the crucial role of a horizontally acquired alginate lyase for brown algal biomass degradation by Zobellia galactanivorans, Environ. Microbiol. 19 (2017) 2164–2181.
[4] K.Y. Lee, D.J. Mooney, Alginate: properties and biomedical applications, Prog. Polym. Sci. 37 (2012) 106–126.
[5] O. Smidsrod, K.I. Draget, Chemistry and physical properties of alginates, Carbohydr. Eur. 14 (1996) 6–13.
[6] P.J. Tatnell, N.J. Russell, J.R. Govan, P. Gacesa, Colonisation of cystic fibrosis patients by non-mucoid Pseudomonas aeruginosa–characterisation of the alginate from mucoid variants, Biochem. Soc. Trans. 24 (1996) 406S.
[7] B.H. Rehm, E. Grabert, J. Hein, U.K. Winkler, Antibody response of rabbits and cystic fibrosis patients to an alginate-specific outer membrane protein of a mucoid strain of Pseudomonas aeruginosa, Microb. Pathog. 16 (1994) 43–51.
[8] S. Leone, A. Molinaro, F. Alfieri, V. Cafaro, R. Lanzetta, A. Di Donato, M. Parrilli, The biofilm matrix of Pseudomonas sp. OX1 grown on phenol is mainly constituted by alginate oligosaccharides, Carbohydr. Res. 341 (2006) 2456–2461.
[9] J. Preiss, G. Ashwell, Alginic acid metabolism in bacteria. I. Enzymatic formation of unsaturated oligosac-charides and 4-deoxy-L-erythro-5-hexoseulose uronic acid, J. Biol. Chem. 237 (1962) 309–316.
[10] B.L. Cantarel, P.M. Coutinho, C. Rancurel, T. Bernard, V. Lombard, B. Henrissat, The Carbohydrate-Active EnZymes database (CAZy): an expert resource for Glycogenomics, Nucleic Acids Res. 37 (2009) D233–D238.
[11] F. Xu, P. Wang, Y.Z. Zhang, X.L. Chen, Diversity of three-dimensional structures and catalytic mechanisms of alginate lyases, Appl. Environ. Microbiol. 84 (2018).
[12] W. Helbert, L. Poulet, S. Drouillard, S. Mathieu, M. Loiodice, M. Couturier, V. Lombard, N. Terrapon, J. Turchetto, R. Vincentelli, B. Henrissat, Discovery of novel carbohydrate-active enzymes through the rational exploration of the protein sequences space, Proc. Natl. Acad. Sci. U. S. A. 116 (2019) 6063–6068.
[13] B. Mikami, M. Ban, S. Suzuki, H.J. Yoon, O. Miyake, M. Yamasaki, K. Ogura, Y. Maruyama, W. Hashimoto, K. Murata, Induced-fit motion of a lid loop involved in

catalysis in alginate lyase A1-III, Acta Crystallogr. D Biol. Crystallogr. 68 (2012) 1207–1216.
[14] H.J. Yoon, W. Hashimoto, O. Miyake, K. Murata, B. Mikami, Crystal structure of alginate lyase A1-III complexed with trisaccharide product at 2.0 A resolution, J. Mol. Biol. 307 (2001) 9–16.
[15] F. Xu, F. Dong, P. Wang, H.Y. Cao, C.Y. Li, P.Y. Li, X.H. Pang, Y.Z. Zhang, X.L. Chen, Novel molecular insights into the catalytic mechanism of marine bacterial alginate lyase AlyGC from polysaccharide lyase family 6, J. Biol. Chem. 292 (2017) 4457–4468.
[16] K. Ogura, M. Yamasaki, B. Mikami, W. Hashimoto, K. Murata, Substrate recognition by family 7 alginate lyase from Sphingomonas sp. A1, J. Mol. Biol. 380 (2008) 373–385.
[17] X.L. Chen, S. Dong, F. Xu, F. Dong, P.Y. Li, X.Y. Zhang, B.C. Zhou, Y.Z. Zhang, B.B. Xie, Characterization of a new cold-adapted and salt-activated polysaccharide lyase family 7 alginate lyase from pseudoalteromonas sp. SM0524, Front. Microbiol. 7 (2016) 1120.
[18] H.M. Qin, T. Miyakawa, A. Inoue, R. Nishiyama, A. Nakamura, A. Asano, Y. Sawano, T. Ojima, M. Tanokura, Structure and polymannuronate specificity of a eukaryotic member of polysaccharide lyase family 14, J. Biol. Chem. 292 (2017) 2182–2190.
[19] K. Ogura, M. Yamasaki, T. Yamada, B. Mikami, W. Hashimoto, K. Murata, Crystal structure of family 14 polysaccharide lyase with pH-dependent modes of action, J. Biol. Chem. 284 (2009) 35572–35579.
[20] A. Ochiai, M. Yamasaki, B. Mikami, W. Hashimoto, K. Murata, Crystal structure of exotype alginate lyase Atu3025 from Agrobacterium tumefaciens, J. Biol. Chem. 285 (2010) 24519–24528.
[21] D. Park, S. Jagtap, S.K. Nair, Structure of a PL17 family alginate lyase demonstrates functional similarities among exotype depolymerases, J. Biol. Chem. 289 (2014) 8645–8655.
[22] S. Dong, T.D. Wei, X.L. Chen, C.Y. Li, P. Wang, B.B. Xie, Q.L. Qin, X.Y. Zhang, X.H. Pang, B.C. Zhou, Y.Z. Zhang, Molecular insight into the role of the N-terminal extension in the maturation, substrate recognition, and catalysis of a bacterial alginate lyase from polysaccharide lyase family 18, J. Biol. Chem. 289 (2014) 29558–29569.
[23] H. Ertesvag, Alginate-modifying enzymes: biological roles and biotechnological uses, Front. Microbiol. 6 (2015) 523.
[24] Y. Cheng, D. Wang, J. Gu, J. Li, H. Liu, F. Li, W. Han, Biochemical characteristics and variable alginate-degrading modes of a novel bifunctional endolytic alginate lyase, Appl. Environ. Microbiol. 83 (2017).
[25] P. Ghadam, F. Akhlaghi, A.A. Ali, One-step purification and characterization of alginate lyase from a clinical Pseudomonas aeruginosa with destructive activity on bacterial biofilm, Iran. J. Basic Med. Sci. 20 (2017) 467–473.
[26] H. Tavafi, A.A. Ali, P. Ghadam, S. Gharavi, Screening, cloning and expression of a novel alginate lyase gene from P. aeruginosa TAG 48 and its antibiofilm effects on P. aeruginosa biofilm, Microb. Pathog. 124 (2018) 356–364.
[27] M. Enquist-Newman, A.M. Faust, D.D. Bravo, C.N. Santos, R.M. Raisner, A. Hanel, P. Sarvabhowman, C. Le, D.D. Regitsky, S.R. Cooper, L. Peereboom, A. Clark, Y. Martinez, J. Goldsmith, M.Y. Cho, P.D. Donohoue, L. Luo, B. Lamberson, P. Tamrakar, E.J. Kim, J.L. Villari, A. Gill, S.A. Tripathi, P. Karamchedu, C.J. Paredes, V. Rajgarhia, H.K. Kotlar, R.B. Bailey, D.J. Miller, N.L. Ohler, C. Swimmer, Y. Yoshikuni, Efficient ethanol production from brown macroalgae sugars by a synthetic yeast platform, Nature 505 (2014) 239–243.
[28] C. Creze, S. Castang, E. Derivery, R. Haser, N. Hugouvieux-Cotte-Pattat, V.E. Shevchik, P. Gouet, The crystal structure of pectate lyase peli from soft rot pathogen Erwinia chrysanthemi in complex with its substrate, J. Biol. Chem. 283 (2008) 18260–18268.
[29] J. Jenkins, V.E. Shevchik, N. Hugouvieux-Cotte-Pattat, R.W. Pickersgill, The crystal structure of pectate lyase Pel9A from Erwinia chrysanthemi, J. Biol. Chem. 279 (2004) 9139–9145.
[30] A. Ochiai, T. Itoh, Y. Maruyama, A. Kawamata, B. Mikami, W. Hashimoto, K. Murata, A novel structural fold in polysaccharide lyases: Bacillus subtilis family 11 rhamnogalacturonan lyase YesW with an eight-bladed beta-propeller, J. Biol. Chem. 282 (2007) 37134–37145.
[31] T. Ulaganathan, E. Banin, W. Helbert, M. Cygler, Structural and functional characterization of PL28 family ulvan lyase NLR48 from Nonlabens ulvanivorans, J. Biol. Chem. 293 (2018) 11564–11573.
[32] M.L. Garron, M. Cygler, Structural and mechanistic classification of uronic acid-containing polysaccharide lyases, Glycobiology 20 (2010) 1547–1573.
[33] Y.Z. Xia, W.Q. Chu, Q.S. Qi, L.Y. Xun, New insights into the QuikChange (TM) process guide the use of Phusion DNA polymerase for site-directed mutagenesis, Nucleic Acids Res. 43 (2015).
[34] S. Doublie, Production of selenomethionyl proteins in prokaryotic and eukaryotic expression systems, Methods Mol. Biol. 363 (2007) 91–108.
[35] R.C. Edgar, MUSCLE: multiple sequence alignment with high accuracy and high throughput, Nucleic Acids Res. 32 (2004) 1792–1797.
[36] T.N. Petersen, S. Brunak, G. von Heijne, H. Nielsen, SignalP 4.0: discriminating signal peptides from transmembrane regions, Nat. Methods 8 (2011) 785–786.
[37] G. Michel, K. Pojasek, Y. Li, T. Sulea, R.J. Linhardt, R. Raman, V. Prabhakar, R. Sasisekharan, M. Cygler, The structure of chondroitin B lyase complexed with glycosaminoglycan oligosaccharides unravels a calcium-dependent catalytic machinery, J. Biol. Chem. 279 (2004) 32882–32896.
[38] P. Wang, X.L. Chen, C.Y. Li, X. Gao, D.Y. Zhu, B.B. Xie, Q.L. Qin, X.Y. Zhang, H.N. Su, B.C. Zhou, L.Y. Xun, Y.Z. Zhang, Structural and molecular basis for the novel catalytic mechanism and evolution of DddP, an abundant peptidase-like bacterial Dimethylsulfoniopropionate lyase: a new enzyme from an old fold, Mol. Microbiol. 98 (2015) 289–301.
[39] T.R. Schneider, G.M. Sheldrick, Substructure solution with SHELXD, Acta Crystallogr. D 58 (2002) 1772–1779.
[40] P. Emsley, K. Cowtan, Coot: model-building tools for molecular graphics, Acta Crystallogr. D Biol. Crystallogr. 60 (2004) 2126–2132.
[41] P.D. Adams, R.W. Grosse-Kunstleve, L.W. Hung, T.R. Ioerger, A.J. McCoy, N.W. Moriarty, R.J. Read, J.C. Sacchettini, N.K. Sauter, T.C. Terwilliger, PHENIX: building new software for automated crystallographic structure determination, Acta Crystallogr. D Biol. Crystallogr. 58 (2002) 1948–1954.